

The Solvent Synthesis, Growth Mechanism, Photocatalytic Properties of AgInS₂ Nanoplate and Nanoparticle

Yue Wang^{1*}, Yongfang Shi^{2*}, Dongwei Li¹, Tao Zhang¹, Xiaochuan Zou¹ and Yucen He¹

¹School of Biological and Chemical Engineering, Chongqing University of Education, Nan'an District, Chongqing, China

²Fujian Institute of Research on the Structure of Matter, Key Laboratory of Research on Chemistry and Physics of Optoelectronic Materials, Chinese Academy of Sciences, Fuzhou, Fujian Province, China

ABSTRACT

Orthorhombic AgInS₂ nanoplate and nanoparticle were synthesized using pyridine and 1-dodecanethiol as the solvent. The obtained products were characterized by X-ray diffraction (XRD), field-emission scanning electron microscope (FESEM), field-emission transmission electron microscope (FETEM), and the possible growth mechanism of AgInS₂ was also proposed by the exploration of reaction temperature and time. Meanwhile, the band gap of AgInS₂ were calculated by the UV-vis diffuse reflectance spectrum, and the photocatalytic activity was also investigated. Those experimental results indicate that the reaction temperature, reaction time and solvent have an influence on the phase and morphology of AgInS₂, and both AgInS₂ nanoplate and nanoparticle have some ability on photocatalytic degradation of organic dyes under visible light irradiation.

Keywords: Orthorhombic AgInS₂, Nanostructure, Solvent method, Growth mechanism, Photocatalysis

INTRODUCTION

With the development of society, people pay more and more attention to the pollution caused by industrial waste water [1]. The semiconductor photocatalytic method, especially using cheap sunlight as the light source, to realize visible photocatalytic degradation of pollutants is a new technology of low energy consumption and environmental protection. As an important I-II-VI group semiconductor material, ternary metal sulfide, AgInS₂, has gradually become a research hotspot, due to its unique photoelectric and catalytic performance, which has potential application prospect in the field of light-emitting diodes, nonlinear optical devices, solar cells, photocatalysis, biological labelling [2-7]. Currently, the preparation methods of AgInS₂ are hot pressing method [8], hot-wall epitaxial growth method [9], hydrothermal method [10], solvothermal method [11], hot injection method [12], and thermolysis method [13], etc. The previous works focus on the 0D AgInS₂ quantum dots, but few studies of 2D and 3D nanostructures [4]. In our previous work [13,14], the metastable orthorhombic AgInS₂ flower-like microsphere was successfully prepared by the pyrolysis of organometallic precursors at 250~280°C. However, considering the high temperature (above 200°C) needs the high energy consumption, and the products should be heated more uniformly in the solvent, as well as the solvent has important influence on the morphology of the product, so we try to disperse the precursor in different solvent to obtain AgInS₂ nanostructures with different morphology at lower temperature. The results indicate that AgInS₂ nanoplate and nanoparticle can be obtained at lower temperature (120~150°C) using pyridine and 1-dodecanethiol as the solvent. Meanwhile, the obtained products were characterized by X-ray diffraction (XRD), field-emission scanning electron microscope (FESEM), field-emission transmission electron microscope (FETEM), and the possible growth mechanism of AgInS₂ was also proposed by the exploration of reaction temperature and time. Finally, the bandgap of AgInS₂ were calculated by the UV-vis diffuse reflectance spectrum, and the photocatalytic activity was also investigated, as well as its possible photocatalytic mechanism.

MATERIALS AND METHODS

Experimental

Chemicals

Silver nitrate (AgNO_3), indium nitrate hydrate ($\text{In}(\text{NO}_3)_3 \cdot 4.5\text{H}_2\text{O}$), carbon disulfide (CS_2), potassium hydrate (KOH), ethanol ($\text{C}_2\text{H}_5\text{OH}$), chloroform (CHCl_3), dichloromethane (CH_2Cl_2), and pyridine ($\text{C}_5\text{H}_5\text{N}$), dichloromethane (CH_2Cl_2), 1-dodecanethiol ($\text{C}_{12}\text{H}_{25}\text{SH}$), ethylenediamine ($\text{C}_2\text{H}_8\text{N}_2$), and oleic acid ($\text{C}_{18}\text{H}_{34}\text{O}_2$) were purchased from Shanghai Chemical Co.. $[\text{CH}_3(\text{CH}_2)_7]_2\text{NH}$ (Alfa, A.R.) was used. All reactants were used as received.

Synthesis of $\text{Ag}(\text{OTC})$ and $\text{In}(\text{OTC})_3$ Precursors

Precursors were prepared according to the reactions shown in **Scheme 1**. Below 0°C , CS_2 had reacted with $[\text{CH}_3(\text{CH}_2)_7]_2\text{NH}$ and KOH to produce enough dithiocarbamate salt in ethanol (**Reaction 1**). Then, an ethanol solution with excess $\text{In}(\text{NO}_3)_3 \cdot 4.5\text{H}_2\text{O}$ was added to generate white suspension $\text{In}[\text{S}_2\text{CN}(\text{C}_8\text{H}_{17})_2]_3$ (**Reaction 2**). After stirring for 5 min, an ethanol solution with an appropriate amount of AgNO_3 with a mole ratio of $\text{M}^+:\text{In}^{3+} = 1:1.25$ was added and stirred for another 2 h to ensure the complete reaction to form $\text{In}(\text{OTC})_3$ and $\text{Ag}(\text{OTC})$ precursors (**Reaction 3**) and make them mix evenly. A solid was obtained after the rotary evaporation of ethanol and then dissolved in CHCl_3 and filtrated. Then, this CHCl_3 -filtration was rotary evaporated to generate the $\text{Ag}(\text{OTC})/\text{In}(\text{OTC})_3$ precursor, a soil-like solid. Finally, the precursors were washed by acetone. The precursor color is yellow.

Synthesis of the AgInS_2

In a typical process, the precursor was added into a solution containing pyridine or other solvents. The mixture was stirred for 15 min at room temperature in air, and then poured into a 25 ml Teflon-lined stainless autoclave. The autoclave was heated at $120\sim 150^\circ\text{C}$ for 17.5~20 h under autogenous pressure, and then air-cooled to room temperature. The resulting precipitates were collected and washed with CH_2Cl_2 and ethanol thoroughly and dried at room temperature in air. The AgInS_2 product is dark red.

Characterization

X-ray powder diffraction (XRD), transmission electron microscopy (TEM), high-resolution TEM (HRTEM), and scanning electron microscopy (SEM) were used to characterize the structure, composition, size, and shape of the synthesized nanoproducs, respectively. The XRD patterns were collected with the aid of a PANalytical X'Pert Pro diffractometer at room temperature, at 40 kV and 40 mA with $\text{Cu K}\alpha$ radiation. The TEM images were obtained using a JEM 2010 TEM equipped with a field emission gun operating at 200 kV. Images were acquired digitally using a Gatan multipole scanning CCD camera with an imaging software system. The EDX analyses were performed on a carbon-film-coated Cu grid with the aid of a JEM 2010 TEM equipped with an Oxford INCA spectrometer. The optical diffuse reflectance spectrum was measured at room temperature using a Perkin-Elmer Lambda 900 UV-vis spectrophotometer equipped with an integrating sphere attachment and BaSO_4 as reference. The UV-vis spectra were measured on a Perkin-Elmer Lambda-35 spectrophotometer.

Photocatalytic activity test

The photocatalytic activities of the samples were investigated by the decomposition rate of methyl orange (MO) or Methylene blue (MB) in an aqueous solution under UV-vis light irradiation. Briefly, 100 mg of AgInS_2 nano powders was dispersed in 100 mL of MB or MO solution with an initial concentration of 10 ppm. Prior to irradiation, the suspension was stirred in the dark for 1 h to ensure the establishment of the adsorption-desorption equilibrium. The assembly was continuously stirred and irradiated by a 300 W halogen-tungsten lamp. At an irradiation time interval of 1 h, 4 mL of the suspension was collected and then the slurry samples including the photocatalyst and MO or MB solution were centrifuged to remove the photocatalyst particles. The concentration of MO or MB was analyzed by measuring the absorbance at 664 nm wavelength for MB (or 463 nm wavelength for MO) using a UV-VIS spectrophotometer.

RESULTS AND DISCUSSION

Phase and microstructure

The XRD patterns of the as-synthesized products prepared using pyridine as the solvent at 120°C for 20 h (**Figure 1a**) and using 1-dodecanethiol as the solvent at 150°C for 17.5 h (**Figure 1b**) can be indexed to the ICDD pattern (PDF#25-1328). We can see that the position of all the diffraction peaks corresponds to (120), (002), (121), (202), (320), (123) and (322) plane and are in agreement with the orthorhombic phase of AgInS₂. The difference between those patterns is that the intensity of (002) plane in **Figure 1a** is much higher than one in **Figure 1b**, which is probably due to their different morphology.

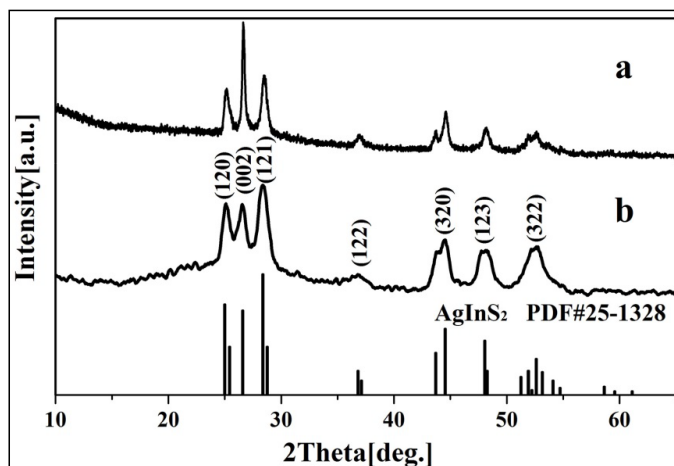


Figure 1: XRD pattern of as-prepared AgInS₂ samples: (a) 120°C/20 h, pyridine as the solvent; (b) 150°C/17.5 h, 1-dodecanethiol as the solvent.

As shown in **Figures 2a** and **2b**, the AgInS₂ produced in pyridine at 120°C for 20 h are nanoplates with width of 300~500 nm, and thickness of about 40 nm, which are stacked and not well dispersed. However, AgInS₂ produced in 1-dodecanethiol at 150°C for 17.5 h are irregular nanoparticles (SEM: **Figure 2c**), which is severely agglomerated and the dispersity is still not well even after ultrasonic concussion (TEM: **Figure 2d**). Comparing with 0D nanoparticle, the 2D nanoplate takes a preferred orientation for powder diffraction, so the intensity of (002) diffraction peak is greatly increased, which also explains why the peak in **Figure 1a** is significantly higher than that in **Figure 1b**. A typical HRTEM image of the edge of such a nanoparticle is shown in **Figure 2e**, indicating the size of those particles is about 14 nm (calculated by the red circle). Clear lattice fringes (**Figure 2f**) can be observed after FFT inversion and the single-crystal natures of the nanoparticles are revealed. The interplanar spacing is about 0.357 nm, in good agreement with the distance (0.356 nm) of (120) planes of orthorhombic AgInS₂.

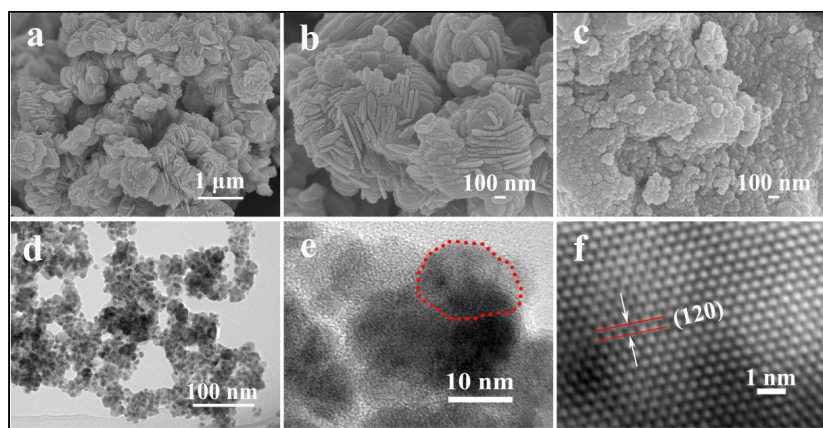


Figure 2: (a, b) SEM images of AgInS₂ samples prepared at 120°C for 20 h, using pyridine as the solvent; (c, d) SEM and TEM images of AgInS₂ samples prepared at 150°C for 17.5 h, using 1-dodecanethiol as the solvent; (e, f) HRTEM images of particle in picture d, indicating that the size of particle is about 14 nm (calculated by the red circle), and the interplanar spacing is 0.357 nm, in good agreement with the distance (0.356 nm) of (120) planes of orthorhombic AgInS₂.

Using pyridine as the solvent, we can observe the formation of orthorhombic AgInS₂ by adjusting the reaction time under the condition of 120°C. When the reaction time was 5 h, a small amount of Ag₂S (**Figure 3a**) with weak diffraction peak of XRD was obtained, and there were only two obvious peaks; when the reaction time was increased to 10 h, the peak intensity of XRD (**Figure 3b**) had significantly enhanced, in good agreement with that of monoclinic Ag₂S (ICDD PDF# 14-0072). It can be seen from **Figure 3d** that the Ag₂S also contains two morphologies, namely, the hexagon with a length of about 100 nm and the particle with size of about 50 nm, and the amount of particles is significantly more than the hexagon. When the reaction time was further extended to 15 h, the obvious diffraction peak of orthorhombic AgInS₂ appeared (**Figure 3c**), and its intensity is higher than that of Ag₂S, indicating that most of the Ag₂S have been transformed into AgInS₂. Furthermore, the amount of the original small particles greatly reduced, but both the number and size of the hexagonal sheet increased (**Figure 3e**). This result shows that, as the reaction time is increased, the newly generated monoclinic Ag₂S gradually transforms into orthorhombic AgInS₂, accompanied by the transformation from particles to hexagonal plate. This point can be verified that pure orthorhombic AgInS₂ nanoplates are obtained when the reaction time is extended to 20 h (**Figures 1a and 2a**).

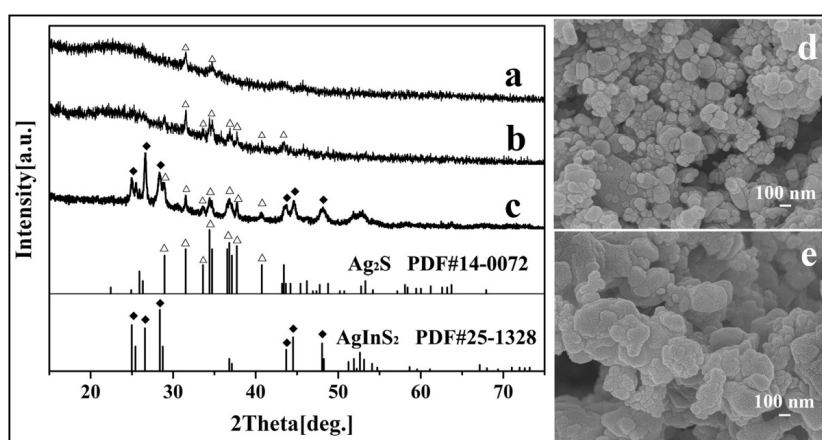
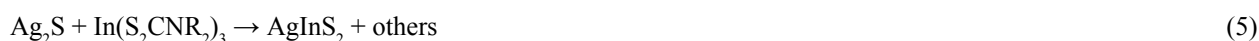
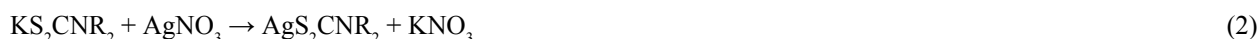


Figure 3: XRD patterns and SEM images of products prepared at 120°C for different time: (a) 5 h, weak diffraction peak, monoclinic Ag₂S; (b,d) 10 h, monoclinic Ag₂S, similar quantity of nanoplate and nanoparticle; (c,e) 15 h, the major orthorhombic AgInS₂ with minor monoclinic Ag₂S, and the quantity of nanoplate is much larger than nanoparticle.

According to the above experimental facts, combined with the previous work [15] and results obtained by our group [16,17], we has proposed the possible growth mechanism of orthorhombic AgInS₂, and the reactions are as follows (HNR₂, R= -C₈H₁₇):



Scheme 1: Reactions to generate AgInS₂

The as-prepared KS₂CNR₂ (**Reaction 1**) was coordinated with Ag⁺ and In³⁺ to form the corresponding complex AgS₂CNR₂ (**Reaction 2**) and In(S₂CNR₂)₃ (**Reaction 3**). Since these complexes were formed in solution and have been fully stirred, it should not be a simple mechanical mixture in the final solid form, but rather a uniform mixture at the molecular level. As the reaction temperature increased, AgS₂CNR₂ began to decompose into corresponding Ag₂S (**Reaction 4**), because Ag⁺ has a high diffusivity under high temperature, which can move freely in the lattice of cation hole [18]. Therefore, In³⁺, released slowly from In(S₂CNR₂)₃, can replace part of Ag⁺ in the Ag₂S lattice, leading to form orthorhombic AgInS₂ gradually (**Reaction 5**). On the other hand, when using pyridine as the solvent, the as-prepared Ag₂S particles wrapped by pyridine, would grow anisotropically into lamellar structure; while using

1-dodecanethiol as the solvent, the as-prepared Ag_2S particles wrapped by 1-dodecanethiol, would grow isotropically into irregular particle with small size. Hence, when the In^{3+} partially replaces the Ag^+ in the Ag_2S lattice, it will not change the morphology, and finally the product grows into nanoplates or nanoparticles, respectively.

Effect of reaction temperature

In order to investigate the morphology-reaction temperature relationship, a batch of parallel reactions using pyridine as the solvent has been carried out, and some representative SEM images are displayed. The detailed experimental results are listed in **Table 1**. The results indicated that when temperature is increased to 150°C , the products are also pure orthorhombic AgInS_2 nanoplate (XRD: **Figure 4a**, SEM: **Figure 5a**), similar to that of 120°C ; while at 170°C , besides of orthorhombic AgInS_2 , minor tetragonal AgInS_2 (ICDD PDF# 25-1330) begins to appear, and lots of nanoparticles are observed (XRD: **Figure 4b**, SEM: **Figure 5b**), indicating that some orthorhombic AgInS_2 has transformed into tetragonal AgInS_2 , namely metastable phase transforms into stable phase [19], so the morphology of products takes an obvious change. When the temperature continues to rise to 190°C , the relative intensity of the diffraction peak of tetragonal phase is not significantly improved (**Figure 4c**), showing that the percentage of tetragonal phase has not significantly enhanced. The products are also nanoparticles similar to that of 170°C , but almost none of nanoplate is observed (**Figure 5c**).

Table 1: Products synthesized using pyridine as the solvent at different temperature.

Temperature ($^\circ\text{C}$)	Time (h)	XRD	Phase	SEM	Morphology
150	17.5	Figure 4a	orthorhombic AgInS_2	Figure 5a	nanoplate
170	17.5	Figure 4b	orthorhombic AgInS_2 + tetragonal AgInS_2 (minor)	Figure 5b	nanoplate (minor) + nanoparticle
190	17.5	Figure 4c	orthorhombic AgInS_2 + tetragonal AgInS_2 (minor)	Figure 5c	nanoparticle

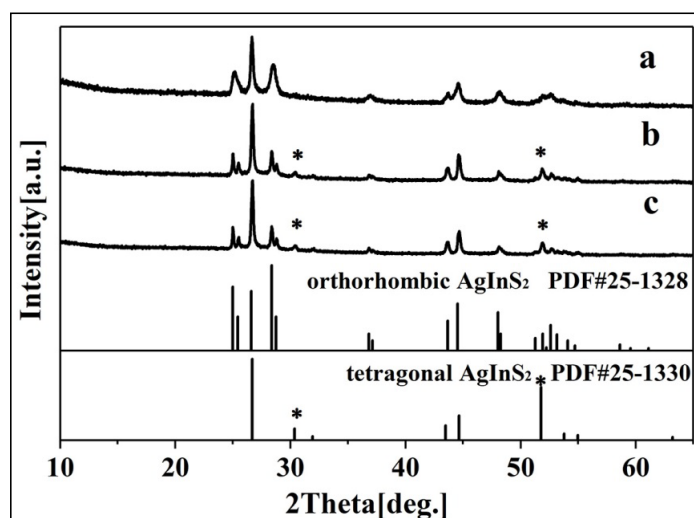


Figure 4: XRD patterns of products prepared at different temperature for 17.5 h using pyridine as the solvent: (a) 150°C , orthorhombic AgInS_2 ; (b) 170°C , orthorhombic AgInS_2 (major) + tetragonal AgInS_2 (minor); (c) 190°C , orthorhombic AgInS_2 (major) + tetragonal AgInS_2 (minor)

Therefore, using pyridine as the solvent, the optimal temperature range to synthesize orthorhombic AgInS_2 nanoplate is $120\sim 150^\circ\text{C}$, and the optimal range of reaction time is $17.5\sim 20$ h. If the temperature is too low or the time is too short, the samples should not fully react to produce pure ternary sulfide AgInS_2 . However, the higher temperature will make metastable AgInS_2 transform into tetragonal AgInS_2 . It is interesting to find that when 1-dodecanethiol is used as the solvent, the orthorhombic AgInS_2 can be obtained at $120\sim 190^\circ\text{C}$ for $17.5\sim 20$ h, which indicates that the solvent also plays a certain role in the formation of AgInS_2 .

Effect of the solvent

To further understand the effect of the solvent, some other solvents are used instead of pyridine and 1-dodecanethiol. All these parallel reactions have been run at 150°C for 17.5 h. The detailed experimental results are listed in **Table 2**. When using ethylenediamine as the solvent, the product is a mixture containing lots of orthorhombic AgInS_2 and

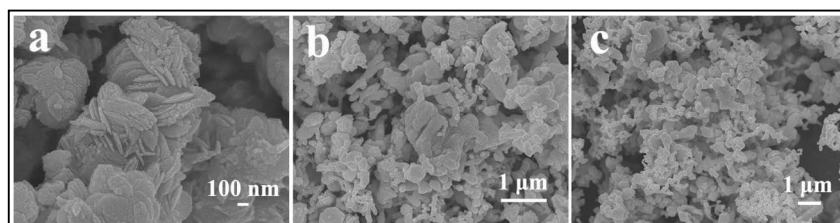


Figure 5: SEM images of products prepared at different temperature for 17.5 h using pyridine as the solvent: (a) 150°C; (b) 170°C; (c) 190°C.

Table 2: Products synthesized using other solvents at 150°C for 17.5 h.

Sample	Solvent	XRD	Phase	SEM	Morphology
1	Ethylenediamine	Figure 6a	orthorhombic AgInS ₂ + tetragonal AgInS ₂ (minor)	Figure 6c	square nanoplate + particle (minor)
2	Oleic acid	Figure 6b	orthorhombic AgInS ₂ + monoclinic Ag ₂ S	Figure 6d	particle

a small amount of tetragonal AgInS₂ (XRD: **Figure 6a**); besides of a small number of particles, most of products are square sheet with the thickness of 30~60 nm (SEM: **Figure 6c**). While using oleic acid as the solvent, both orthorhombic AgInS₂ nanoparticles and monoclinic Ag₂S nanoparticles are observed (XRD: **Figure 6b**; SEM: **Figure 6d**), indicating that 150°C is too low, or 17.5 h is too short for as-prepared Ag₂S completely transforms to AgInS₂, which may be due to the strong adsorption properties of oleic acid. The oleic acid can be firmly adsorbed on the surface of as-prepared Ag₂S particles, which may hinder In³⁺ to replace the Ag⁺, leading the conversion rate is greatly reduced, so it requires higher temperature or longer time to complete the transformation. This result shows that the solvent has a great influence on the phase and morphology of the products.

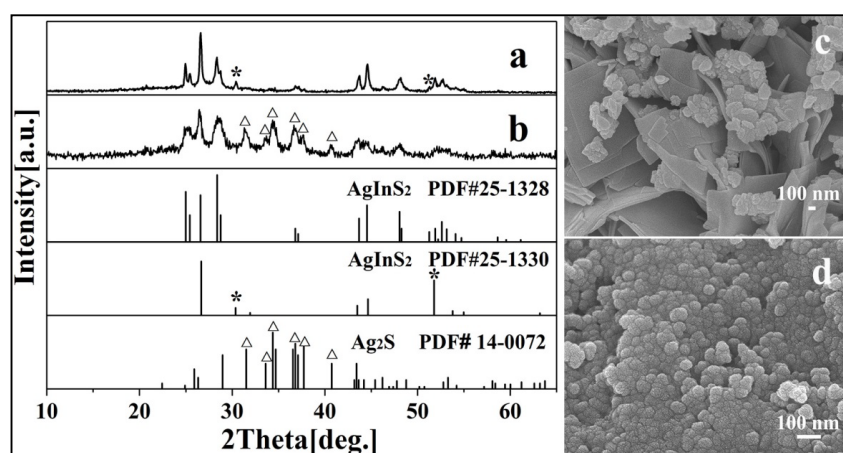


Figure 6: XRD patterns and SEM images of products prepared at 150°C for 17.5 h using other solvents: (a,c) ethylenediamine, orthorhombic AgInS₂ + tetragonal AgInS₂ (minor), square nanoplate + particle (minor); (b, d) oleic acid, orthorhombic AgInS₂ + monoclinic Ag₂S, nanoparticle.

UV-VIS diffuse reflectance spectroscopy

For I-III-VI family compounds, most of them are direct-narrow-gap semiconductors with chalcopyrite structure [20]. AgInS₂ has chalcopyrite and orthorhombic phases, and the band gap values are 1.87 and 1.98 eV, respectively [21-23]. Because of its suitable bandgap, it has a good absorption in the visible range, so it is a good photocatalytic material. Fig.7 is the solid UV-vis diffuse reflectance spectra of AgInS₂ nanoplates and AgInS₂ nanoparticles. The band gap of AgInS₂ can be calculated according to the Equation 1[24]:

$$\alpha h\nu = (h\nu - E_g)^n \quad (1)$$

Here, α means absorption coefficient; $h\nu$ means photoelectron energy; the value of n is 1/2 for indirect bandgap compounds, while 2 for direct bandgap compounds, and E_g means bandgap. Taking $h\nu$ as the abscissa, with $(\alpha h\nu)^{1/n}$ as ordinate, the curve is extended to intersect with the abscissa, and the bandgap can be calculated. As seen in **Figure**

7a, the bandgap of AgInS₂ nanoplate is about 1.61 eV, close to the literature report of 1.58~1.63 eV[4,10,24]; while the bandgap of AgInS₂ nanoparticle is about 1.98 eV (**Figure 7b**), consistent with the band gap of AgInS₂ crystal. The difference between the two gaps is probably caused by the different particle sizes. Because the nanoplate has the larger size (thickness about 40 nm, width 300~500 nm), while the nanoparticle is only about 14 nm, which results in the blue shift of the absorption edge due to small size effect.

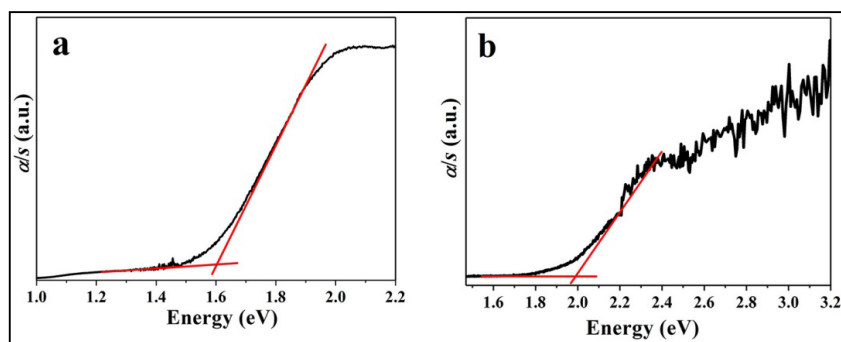


Figure 7: UV-vis diffuse reflectance spectrum of as-prepared products: (a) AgInS₂ nanoplate, synthesized at 120°C for 20 h using pyridine as the solvent, the bandgap is about 1.61 eV; (b) AgInS₂ nanoparticle, synthesized at 150°C for 17.5 h using 1-dodecanethiol as the solvent, the bandgap is about 1.98 eV.

Photocatalytic activity of the AgInS₂ samples

The photocatalytic activities of AgInS₂ samples are measured on the degradation of methyl blue (MB) or methyl orange (MO) in water under UV-vis light irradiation. As shown in **Figure 8a**, with the advance of illumination time, the absorbance of MB in the solution is getting smaller and smaller, indicating that the concentration of MB is lower and lower. After 300 min of irradiation, the conversion of MB by AgInS₂ nanoparticles is about 66% (**Figure 8b**, red curve). However, the conversion of MO by AgInS₂ nanoplates is about 25% (**Figure 8b**, blue curve). The results show that AgInS₂ has the certain ability on photocatalytic degradation of organic dyes such as MB, and it is probably that

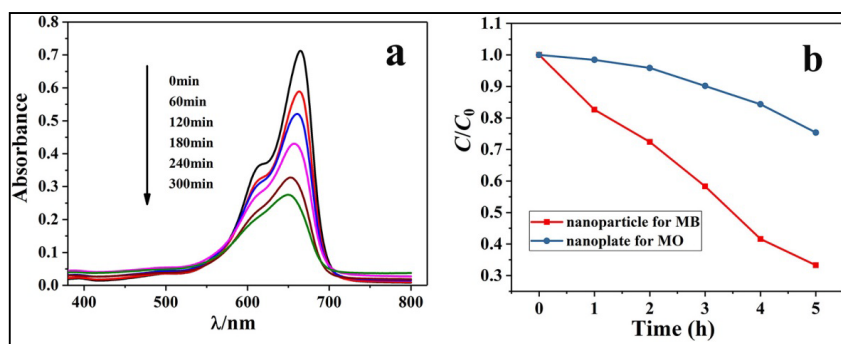


Figure 8: (a) Absorption spectra of MB photocatalytically degraded by AgInS₂ nanoparticle; (b) The relation between MB concentration and time photocatalytically degraded by AgInS₂ nanoparticle (the red curve), and the relation between MO concentration and time photocatalytically degraded by AgInS₂ nanoplate (the blue curve).

the low-power tungsten halogen lamp (300 W) used in the experiment causes unexciting conversion. The possible mechanism on photocatalytic degradation of MB by AgInS₂ can be explained by the following **Scheme 2**:



Scheme 2: The possible mechanism on photocatalytic degradation of MB by AgInS₂[25]

Under visible-light irradiation, the electrons transfer from valance band (VB) of AgInS₂ to the conduction band (CB), while the holes (h^+) generate in its VB (**Reaction 6**). The photogenerated electrons (e^-) can react with adsorbed O₂ to

produce $\bullet\text{O}^{2-}$ (**Reaction 7**) and H_2O_2 (**Reaction 8**). H_2O_2 can further reacts with $\bullet\text{O}^{2-}$ and e^- to generate hydroxyl radicals ($\bullet\text{OH}$) (**Reaction 9**). All of $\bullet\text{O}_2^-$, h^+ and $\bullet\text{OH}$ play a role in the degradation and mineralization of MB (**Reaction 10**).

CONCLUSION

Two kinds of orthorhombic AgInS_2 nanostructures with different morphologies have been successfully prepared by the solvent method using KS_2CNR_2 , AgNO_3 , and $\text{In}(\text{NO}_3)_3$ as reagents. When using pyridine as the solvent, by tuning the reaction temperature and reaction time, it is found that pure AgInS_2 nanoplates with relatively uniform morphology can be obtained at 120~150°C for 17.5~20 h; when the temperature is below 120°C or the reaction time is less than 10 h, most of the product is binary monoclinic Ag_2S , while there will be another ternary tetragonal AgInS_2 generated over 170°C. When using 1-dodecanethiol as the solvent, pure AgInS_2 nanoparticles with size of about 14 nm have been obtained at 120~190°C for 17.5~20 h, indicating that the solvent has a great influence on the phase and morphology, and this point has also been verified using ethylenediamine or oleic acid as the solvent. On the other hand, UV-vis diffuse reflectance spectra show that the bandgap of AgInS_2 nanoplates (1.61 eV) with larger size is less than that of AgInS_2 nanoparticles (1.98 eV) with smaller size, which is likely to be caused by the blue shift of the absorption edge due to the small size effect. Furthermore, the photocatalytic experiments show that AgInS_2 has certain ability on photocatalytic degradation of organic dyes such as MB.

ACKNOWLEDGEMENTS

The research was supported by the Natural Science Foundation of Chongqing (Nos. cstc2013jcyjA50033, cstc2015jcyjA0317), the Project Foundation of Chongqing Municipal Education Committee (Nos. KJ1601403, KJ1601412), and the Project Foundation of Chongqing University of Education (Nos. 16xjpt08, JG201715, XK20170210).

CONFLICT OF INTEREST

The authors declare that they have no conflict of interest.

REFERENCES

- [1] Ren NQ, Zhou XJ, Guo WQ, Yang SS (2013) A Review on treatment methods of dye wastewater. *J Chem Ind Eng (China)* 6: 84-94.
- [2] Zeng Z, Wang AQ, Ping LL, Yang JL, Wang QM (2015) Encapsulation of lanthanides in ternary I - III - VI AgInS_2 nanocrystals and their physical properties. *Mater Lett* 141: 225-227.
- [3] Peng SJ, Zhang SY, Zhang SY, Ramakrishna S (2012) Synthesis of AgInS_2 nanocrystal ink and its photoelectrical application. *Phys Chem* 14: 8523-8529.
- [4] Zou XJ, Dong YY, Rang CQ, Cui YB, Chen Zb (2016) Fabrication of Flower-like AgInS_2 Microsphere and Its Photocatalytic Reduction of Cr(VI). *JWuhanUniv (Nat Sci Ed)* 62: 92-96.
- [5] Bu CF, Liu LW, Wang Q, Zhang BT, Hu SY, et al. (2015) Folic Acid-conjugated AgInS_2 Quantum Dots for in vitro Cancer Cell Imaging. *Chin J Lumin* 36: 989-995.
- [6] Théo C, Gilles LB, Frédéric C (2016) Photoluminescence properties of AgInS_2 -ZnS nanocrystals: the critical role of the surface. *Nanoscale* 8: 7612-7620.
- [7] Azam ES (2014) Photocatalytic oxidation of cyanide under visible light by Pt doped AgInS_2 nanoparticles. *J Ind Eng Chem* 20: 4008-4013.
- [8] Yoshino K, Komaki H, Kakeno T, Akakia Y, Ikaria T (2003) Growth and characterization of p-type AgInS_2 crystals. *J Phys Chem Solids* 64: 1839-1842.
- [9] You SH, Hong KJ, Lee BJ, Jeong TS, Younb CJ, et al. (2002) Temperature dependence of band gap and photocurrent properties for the AgInS_2 epilayers grown by hot wall epitaxy. *J Cryst Growth* 245: 261-266.
- [10] Wei QL, Zhao XL, Yao PP, Mu J (2011) Preparation and Visible Light Photocatalytic Activity of AgInS_2 Nanoparticles. *Chin J Inorg Chem* 27: 692-694.

-
- [11] Kharkwal AN, Jain K, Tyagi SB, Kharkwal M (2015) Novel synthesis of selective phase-shape orientation of AgInS₂ nanoparticles at low temperature. *Colloid Polym Sci* 293: 1953-1959.
- [12] Do YR, Hong SP, Park HK, Ji HO, Yang H, et al. (2012) Comparisons of the structural and optical properties of o-AgInS₂, t-AgInS₂ and c-AgIn₅S₈ nanocrystals and their solid-solution nanocrystals with ZnS. *J Mater Chem* 22: 18939-18949.
- [13] Torimoto T, Adachi T, Okazaki K, Sakuraoka M, Shibayama T, et al. (2007) Facile synthesis of ZnS-AgInS₂ solid solution nanoparticles for a color-adjustable luminophore. *J Am Chem Soc* 129: 12388-12389.
- [14] Wang Y, Zou XC, Wang C, Shi YF (2016) Thermolysis Synthesis and Growth Mechanism of Metastable MInS₂ (M=Ag, Cu) Flowerlike Microsphere. *Chin J Inorg Chem* 32: 2151-2157.
- [15] Zou ZG, Gap Y, Long F, Zhang J (2015) Synthesis and Mechanism of Wurtzite CuInS₂ Nanocrystals. *J Synth Cryst* 44: 2164-2170.
- [16] Shi YF, Wang Y, Wu LM (2013) Hexagonal MIn₂S₄ (M = Mn, Fe, Co): Formation and phase transition. *J Phys Chem C* 117: 20054-20059.
- [17] Fang F, Chen L, Chen Y B, Wu LM (2010) Synthese and Photocatalysis of ZnIn₂S₄ nano/micropeony. *J Phys Chem C* 114: 2393-2397.
- [18] Lu X, Zhuang Z, Peng Q, Li Y (2011) Controlled synthesis of wurtzite CuInS₂ nanocrystals and their side-by-side nanorod assemblies. *CrystEngComm* 13(12): 4039-4045.
- [19] Delgado G, Mora A J, Pineda C, Tinoco T (2001) Simultaneous Rietveld refinement of three phases in the Ag-In-S semiconducting system from X-ray powder diffraction. *Mater Res Bull* 36: 2507-2517.
- [20] Xie CP, Xiang WD, Luo L, Zhong JS, Zhao BY, et al. (2014) Advances on AgInS₂ quantum dots. *J Funct Mater* 45: 4009-4016.
- [21] Hu JQ, Lu QY, Tang KB, Liu XM (1999) Solvothermal reaction route to nanocrystalline semiconductors AgMS₂ (M=Ga, In). *Chem Commun* 12: 1093-1094.
- [22] Aguilera MLA, Hernández JRA, Trujillo MAG, López MO, Puente GC (2007) Photoluminescence studies of chalcopyrite and orthorhombic AgInS₂ thin films deposited by spray pyrolysis technique. *Thin Solid Films* 515: 6272-6275.
- [23] Aguilera MLA, Ortega-López M, Resendiz VMS, Hernández JA, Trujillo MAG (2003) Some physical properties of chalcopyrite and orthorhombic AgInS₂ thin films prepared by spray pyrolysis. *Mater Sci Eng B* 102: 380-384.
- [24] Li XM, Niu JZ, Shen HB, Li LS (2010) Shape controlled synthesis of tadpole-like and heliotrope seed-like AgInS₂ nanocrystals. *Cryst Eng Comm* 12: 4410-4415.
- [25] Deng F, Zhong F, Hu P, Pei XL, Luo XB, et al. (2017) Fabrication of In-rich AgInS₂ nanoplates and nanotubes by a facile low-temperature co-precipitation strategy and their excellent visible-light photocatalytic mineralization performance. *J Nanopart Res* 19: 14.